ACS Energy LETTERS

http://pubs.acs.org/journal/aelccp

VIEWPOINT

# Impact of Semiconductor Band Tails and Band Filling on Photovoltaic Efficiency Limits

Cite This: *ACS Energy Lett.* 2021, 6, 52−57

Read Online

ACCESS | Metrics & More | Article Recommendations | Supporting Information



Since the seminal work of Shockley and Queisser, assessing the detailed balance between absorbed and emitted radiative fluxes from a photovoltaic absorber has been the standard method for evaluating solar cell efficiency limits.[1−3] The principle of detailed balance is one dictated by reciprocity and steady state, so that photons can be absorbed and emitted with equal probability. This basic principle has also been extended to evaluate the effects of multiple junctions,[4,5] hot carriers,[6,7] nanostructured geometries,[8,9] multiexciton generation,[10,11] subunity radiative efficiency,[12] and many other solar cell configurations and nonidealities to estimate limiting efficiencies via modifications to the detailed balance model.

Another important modification to the Shockley−Queisser model is to examine the assumption of an abrupt, step-like onset of the density of electronic states and absorption coefficient. Specifically, it has long been recognized from spectroscopic measurements of semiconductors that band edges are often not abrupt and that the density of states and absorption functions can be characterized by a band tail. This was first recognized by Urbach,[13] who found the absorption coefficient for a variety of materials below their bandgaps to be characterized by an exponential tail:

$$\alpha(E < E_g) = \alpha_0 \exp\left(\frac{E - E_g}{\gamma}\right) \tag{1}$$

where $\alpha_0$ is the absorption coefficient value at the energy of the bandgap; $E_g$ is the bandgap of the material, and $\gamma$ is referred to as the Urbach parameter, which describes the rate at which the absorption coefficient goes to zero. The magnitude of the Urbach parameter can be influenced by impurities and disorder and is typically attributed to fluctuations in the electrostatic potential within a semiconductor. Urbach tails have been observed in a wide range of absorber materials including amorphous, organic, perovskite, II−VI, III−V, and group IV semiconductors.[14−20] While the Urbach exponential tail is the most prominent functional form observed for band tail states, other forms such as Gaussian band tails have been reported, and different functional forms have been attributed to the underlying physics of those systems.[21] In most cases, the band tail can be characterized by an exponential with an argument raised to some power.

Recent detailed balance analyses have also suggested how this important effect, *i.e.* a departure from a step-like absorbance spectra, can also degrade the limiting efficiency of solar cells.[2,20,22−25] However, a key element missing from previous analyses of photovoltaic efficiency is the effect of band filling for semiconductors with nonabrupt band edges, wherein the electron−hole quasi-Fermi level splitting can thereby modify the absorption spectrum and therefore the radiative emission spectrum as well. This voltage-dependent absorption effect was first recognized by Parrott[26] as being necessary to make the detailed balance formulation self-consistent. Perhaps the most intuitive description of why this is necessary is found by examining the generalized Planck's law:[27]

$$S_{PL}(E) = a(E) S_{bb}(E, \Delta\mu) \tag{2}$$

where

$$S_{bb}(E, \Delta\mu) = \frac{2\pi}{h^3 c^2} \frac{E^2}{\exp\left(\frac{E - \Delta\mu}{kT}\right) - 1} \tag{3}$$

and $S_{PL}(E)$ describes the luminescence flux, $a(E)$ is the absorbance, $E$ is the photon energy, $\Delta\mu$ is the quasi-Fermi level splitting, $h$ is Planck's constant, and $c$ is the speed of light. A clear singularity occurs at $E = \Delta\mu$, which is typically ignored in detailed balance calculations because for a step-like absorbance function, we have $E \geq E_g > \Delta\mu$. As a result, the $-1$ in the denominator is neglected and Boltzmann statistics are assumed. Clearly, the situation must change if we consider energies $E < E_g$, as is the case when band tails affect the luminescence spectrum. In this case, the absorptivity must be modified such that $a(E = \Delta\mu) = 0$, and in general the absorption coefficient is occupation dependent:

$$\alpha(E, \Delta\mu) = \alpha_{0K}(E)(f_v - f_c) \tag{4}$$

Where $a_{0K}(E)$ is the absorption coefficient without band-filling and $(f_v - f_c)$ is the band-filling factor.[21,27,28] This contribution of band-filling has also been recognized in experiments as being necessary to accurately fit photoluminescence spectra under high level injection.[29,30] We suggest that this contribution is also important for systems with large band tails, and as an example, we have used this

**Received:** November 10, 2020
**Accepted:** November 19, 2020




https://dx.doi.org/10.1021/acsenergylett.0c02362
*ACS Energy Lett.* 2021, 6, 52−57

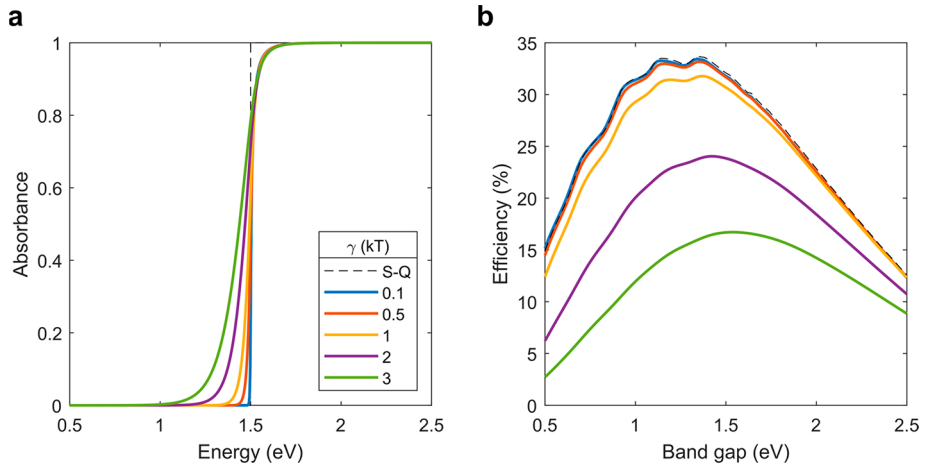


**Figure 1. Effects of band tailing on photovoltaic limiting efficiencies: (a) The spectral absorbance of a photovoltaic cell with a bandgap of $E_g$ = 1.5 eV and a thickness $\alpha_0 L$ = 1 plotted for various Urbach parameters ($\gamma$) in units of $kT$. The dashed line represents the step function absorbance typically used in the Shockley−Queisser (S-Q) limit. (b) The detailed balance efficiencies as a function of the bandgap energy. Different colored lines correspond to different Urbach parameters, with the coloring scheme equal to the legend shown in panel a.**

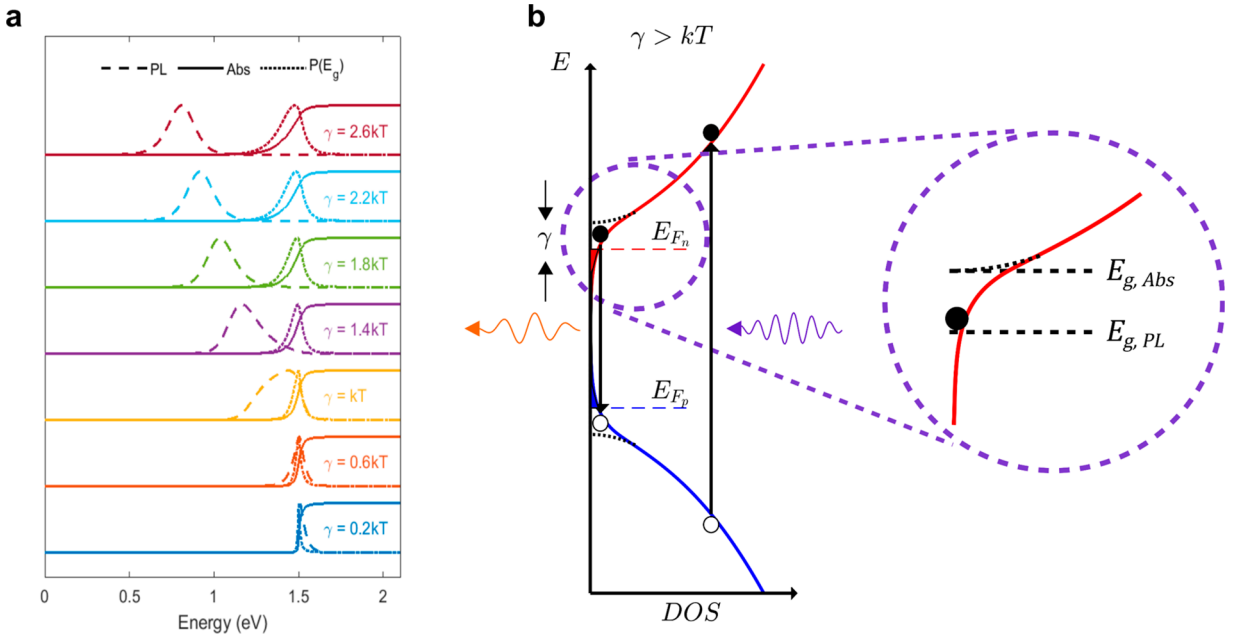


**Figure 2. Effects of band tail states on photoluminescence: (a) The normalized spectral photoluminescence (dashed line) of a photovoltaic cell operating at the radiative limit under 1 sun AM 1.5G illumination for increasing Urbach parameter ($\gamma$) with an offset included for clarity. The corresponding absorbance (solid line) and effective distribution of bandgaps (dotted line) is also plotted, where they are normalized to their peak value. (b) Schematic depiction of the density of states profile along with carrier excitation and recombination; $\gamma$ describes the effective width of the band tail. For small band tailing ($\gamma < kT$), the effect of band tailing is to simply broaden the luminescence peak. For systems with large band tailing ($\gamma > kT$), the luminescence shifts to energies below the nominal absorption band edge.**

modified reciprocity relation to fit the electroluminescence spectrum of a-Si:H which the Rau reciprocity relation[3,31] was previously unable to fit completely (see Figure S1).

*Photovoltaic Efficiency Limit for Semiconductors with Band Tails.* By using the generalized Planck's law (eq 2) and accounting for band filling (eq 4), we can calculate the detailed balance limit for photovoltaic efficiency with band tails in the radiative limit (see Sections S1 and S2 in the Supporting Information). In Figure 1, we consider the case of a band tail parametrized as an exponential Urbach tail and analyze the effects of varying the Urbach parameter. While the spectral response of this modified absorbance appears to be similar to the step function response originally used by Shockley and Queisser (black dashed line), the maximum achievable efficiency drops rapidly from the Shockley−Queisser limit for Urbach parameters larger than the thermal energy, $kT$. These effects are relatively insensitive to the choice of bandgap and thickness (see Figures S2 and S3), and Figure S2 suggests the efficiency drop is primarily due to a voltage loss mechanism.

To analyze the cause of the voltage loss, we examine the luminescence spectrum by using eq 2 and plot these spectra for various Urbach parameters (Figure 2a). In addition, we plot the distribution of bandgaps $P(E_g) = \partial_E \mathrm{Abs}|_{E=E_g}$ proposed by Rau et al.[3] recently, which generalizes the definition of the photovoltaic bandgap for arbitrary absorbance spectra. While the luminescence spectrum is narrow and overlaps significantly


https://dx.doi.org/10.1021/acsenergylett.0c02362
ACS Energy Lett. 2021, 6, 52−57

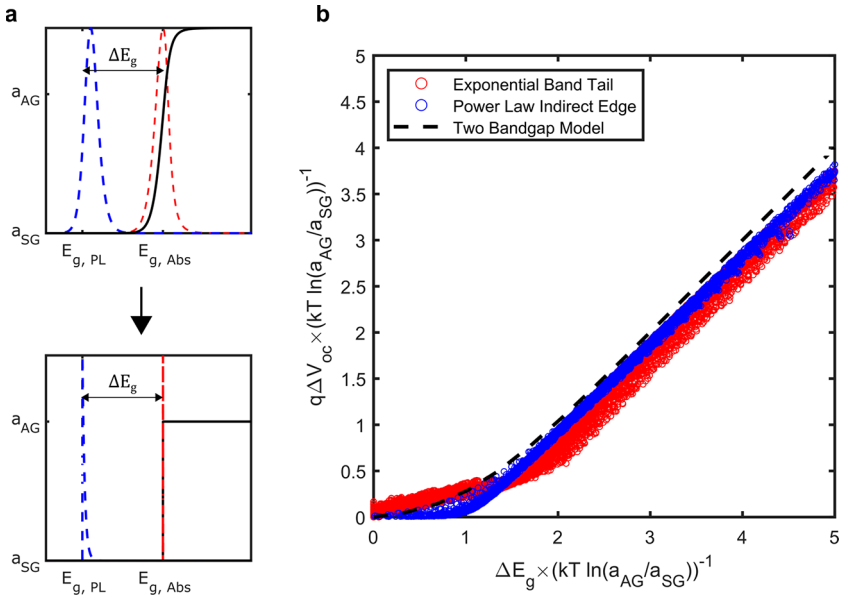


**Figure 3. Generalized voltage losses parametrized as a two-bandgap absorber: (a) Schematic depiction representing a general absorbance and luminescence spectrum as a simpler two-bandgap step function absorbance. Black solid lines are the absorption spectrum, whereas the red dashed line corresponds to the bandgap distribution $P(E_g)$. Blue dashed lines correspond to the luminescence spectrum $S_{PL}$. Typically, $a_{SG} \ll 1$, which is not visible on a linear scale but still contributes to the luminescence spectra because of carrier thermalization. (b) Calculated voltage loss $\Delta V_{oc} = V_{oc,SQ}(E_{g,Abs}) - V_{oc,rad}$ versus observed bandgap shift $\Delta E_g = E_{g,Abs} - E_{g,PL}$, normalized to the energy scale $kT \ln(a_{AG}/a_{SG})$. Every plotted point corresponds to a different absorption spectrum, with $V_{oc,rad}$ calculated using the complete absorption spectra and the full reciprocity relations. The dashed line represents the two-bandgap model, *i.e.*, where we have chosen $\bar{a}_{SG}/\bar{a}_{AG} = 0.1$.**

with the absorption edge for $\gamma < kT$, this is not the case for $\gamma > kT$. In this limit, the luminescence spectrum is significantly broadened and shifts away from the absorption band edge and suggests the definition of a second bandgap, defined by the luminescence spectra. This idea is schematically depicted in Figure 2b, where the absorption bandgap is defined as before, *i.e.* $P(E_{g,Abs}) = \max(P_{E_g})$, while the second bandgap $E_{g,PL}$ is defined by the luminescence spectra $S_{PL}$. We note that this analysis is modified significantly with the inclusion of band-filling effects, which we describe in Sections S3 and S4 and Figures S4 and S5. We also observe the effects of broadening followed by luminescence spectral shifts in band tails parametrized by a Gaussian band tail (Figure S6), where the onset of efficiency loss occurs at approximately $\gamma = 2kT$ instead.

*Generalized Voltage Loss for Semiconductors with Nonabrupt Band Edges.* The similarity between the effects of broadening followed by luminescence shifting for increasing band tail energies suggests a general picture for the voltage loss mechanism, for any band tail functional form. A general trend is the observation of a Stokes shift, *i.e.*, the shift between the absorbance and luminescence spectra, that occurs precisely at the onset of efficiency loss. However, it is unclear whether the voltage loss is just directly proportional to the observed Stokes shift, $\Delta E_g$.

To develop an understanding of this loss mechanism, we consider a simpler absorbance spectrum as a two-bandgap model, represented by the sum of two step function absorbances:

$$a(E) = a_1\theta(E - E_{g,1})\theta(E_{g,2} - E) + a_2\theta(E - E_{g,2}) \quad (5)$$

Here, $a_1$ and $a_2$ are the subgap and above-gap absorbances, respectively, while $\theta(E - E_g)$ is the Heaviside step function, typically considered in the SQ analysis. The photovoltaic bandgap, *i.e.* that defined by absorption, is given by $E_{g,2}$, while $E_{g,1}$ defines the luminescence bandgap. The SQ limit is recovered in the limit that $E_{g,2} \to E_{g,2}$ or $a_1 \to 0$. By varying $a_1$ and $E_{g,1}$ and fixing $E_{g,2}$ to 1.34 eV and $a_2 = 1$, we can analyze the effects of this simple model as we deviate from the SQ limit (see Section S5 and Figure S7 for more details). Interestingly, we find qualitatively similar effects of voltage and efficiency loss in this absorbance model compared to the full effects of the Urbach band tail, albeit parametrized by $a_1$ and $E_{g,1}$ instead of the Urbach parameter $\gamma$. However, we also find that the quantitative bandgap-voltage relation can be significantly affected by the actual functional form used to more accurately model the band tail state distribution, as illustrated in Figure 3.

Nonabrupt band edge absorbances can be mapped onto the two-bandgap model, and therefore, there is a general relation that explains the voltage loss mechanism for any absorbance spectrum given by

$$\Delta V_{oc,rad} = \frac{kT}{q}\ln\left(\frac{\bar{a}_{SG}}{\bar{a}_{AG}}\exp\left(\frac{\Delta E_g}{kT}\right) + 1 - \frac{\bar{a}_{SG}}{\bar{a}_{AG}}\right) \quad (6)$$

where $\bar{a}_{SG}$ is the weighted subgap absorbance and $\bar{a}_{AG}$ is the weighted above-gap absorbance; $\Delta E_g = E_{g,Abs} - E_{g,PL}$ describes the observed Stokes shift between the absorption and luminescence (see definitions in Section S6). Here, $\Delta V_{oc,rad}$ is a voltage loss due *purely* to the nonabruptness of the absorption spectrum, for a semiconductor with assumed unity radiative efficiency. More generally, although nonradiative losses parametrized by a nonunity external radiative efficiency have not been accounted for (see some discussion of radiative efficiency effects in Section S7), band edge nonabruptness by itself can contribute significantly to voltage loss. Indeed, eq 6 results in no net voltage loss as $\Delta E_g \to 0$ and suggests that a finite Stokes shift should be directly correlated to a voltage loss. The magnitude of the voltage loss is scaled by the ratio


https://dx.doi.org/10.1021/acsenergylett.0c02362
ACS Energy Lett. 2021, 6, 52−57

$\bar{a}_{SG}/\bar{a}_{AG}$, and clearly as the ratio approaches 0 or 1, eq 6 recovers the appropriate losses of 0 and $\Delta E_g/q$, respectively.

To observe whether this two-bandgap model can quantitatively describe the more complex band edge functional forms seen in experiments, we choose appropriate definitions for $\bar{a}_{SG}/\bar{a}_{AG}$ and $E_{g,PL}$ and use Rau's definition for $E_{g,Abs}$ (see more details in Sections S6 and S8 and Figure S9). We consider both power law band edges, as a parametrization of indirect band edges, as well as exponential band tails. We find reasonable qualitative agreement but quantitative disagreement between the calculations utilizing the full absorbance spectra and that given by eq 6 (Figure 3b), suggesting that the two-bandgap model is a reasonable first-order representation of the voltage loss mechanism, but importantly, consideration of the actual band tail functional form yields more accurate results. Furthermore, we find that the dimensionless parameter $\xi = \Delta E_g/(kT \ln(\bar{a}_{AG}/\bar{a}_{SG}))$ describes the physical regime of voltage loss. Generally, for $\xi < 1$, voltage loss is minimal because the emission spectrum can be considered as simply a broadening of a single photovoltaic bandgap. In this regime, the efficiency penalty is negligible and generally the detailed balance efficiency limit for $E_{g,Abs}$ can be achieved given sufficient absorption above the photovoltaic bandgap. However, for $\xi > 1$, it is appropriate to define a second bandgap given by the emission spectrum (Figure 3a), resulting in a substantial voltage and efficiency penalty due to additional thermalization losses. Thus, the tuning of the band tail parameter $\gamma$ merely sweeps through different values of $\xi$, and we find that $\xi > 1$ is equivalent to $\gamma > kT$ in the case of an Urbach tail (see Section S5). The discrepancy in eq 6 for large $\xi$ can be attributed to neglecting higher-order terms (see Section S6).

The correlation between the magnitude of the bandgap shift (*i.e.*, $\Delta E_g$) and open-circuit voltage has already been recognized in the organic photovoltaics literature, where the presence of low-energy charge-transfer states generally results in cells with a lower voltage and efficiency.[20,32−35] Here, we have developed a unified picture with an arbitrarily shaped band tail, and by explicitly including band-filling effects, for both large and small band tails, the voltage loss mechanism can be qualitatively captured with a simple two-bandgap model. In addition, by extracting the weighted absorbance ratios, $\bar{a}_{AG}/\bar{a}_{SG}$, we can estimate the voltage losses in the radiative limit using eq 6. We therefore suggest that any radiative transition below the photovoltaic absorption edge $E_{g,abs}$, measurable in luminescence measurements, should result in an efficiency penalty. This efficiency penalty can be viewed as either stemming from a voltage penalty, due to carrier thermalization within the band tails, or equivalently interpreted as being due to incomplete absorption at the lower-energy transition.

To emphasize the implications of these results for various photovoltaic technologies, we have calculated the predicted voltage losses due to a nonabrupt band edge for several different material systems and plotted experimentally measured values for these in Figure 4 (see Table S1 for references and individual data points).[14,20,22] Because Urbach parameters are much more commonly reported than both high-sensitivity EQE and EL spectra, we have used the observed Urbach parameters to calculate the voltage loss directly rather than through eq 6. As expected, we find that semiconductors with large band tails ($\gamma > kT$) or equivalently, large Stokes shifts ($\Delta E_g \gg kT$) have a substantially modified maximum achievable $V_{oc}$, which should be assessed when examining their efficiency potential (e.g., CIGS, a-Si, kesterites, and

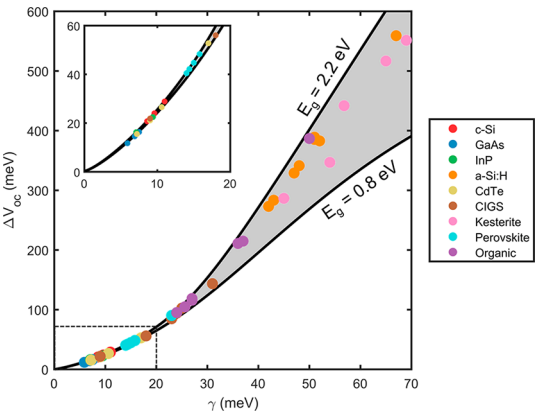


**Figure 4. Voltage loss due to a nonabrupt band edge: Expected open-circuit voltage loss as a function of the observed Urbach parameter $\gamma$, plotted for different materials. The top and bottom black solid lines represent the calculated voltage loss assuming a bandgap of 2.2 and 0.8 eV, respectively. The gray area between the lines represents the voltage loss expected for bandgap values between 0.8 and 2.2 eV, which correspond to most of the materials considered for photovoltaics. The colored data points indicate the expected voltage loss for an experimentally measured Urbach parameter. The dashed line corresponds to the region of the inset, where the voltage loss is minimal and approximately the same irrespective of bandgap.**

OPVs). It should be noted that a more accurate calculation can be made by using the directly measured EQE and EL spectra for a given device.

The analysis presented here should be applicable to any system with nonabrupt band edges that obeys the optoelectronic reciprocity relations and should be employed to evaluate the radiative limits on the open-circuit voltage. We demonstrated here that the voltage dependence of the absorbance or EQE, specifically via band filling, must be included to self-consistently apply the generalized Planck's law for semiconductors. We also suggest that in order to accurately estimate efficiency limits, the abruptness of the band edge should be experimentally characterized by measuring both the absorption and luminescence spectra of photovoltaic materials, and in a completed photovoltaic device, photocurrent and electroluminescence spectra should be used to assess the effects of transport on the reciprocity relations. The magnitude of the voltage loss can then be estimated directly from the spectroscopic measurements by applying reciprocity relations. Additional experimental details and nonidealities for a given photovoltaic material or device may modify the maximum efficiency potential even further, such as reduction in the external radiative efficiency or the finite mobility of charge carriers. However, our analysis suggests the important role that band edge abruptness and band filling can play in defining the limit on open-circuit voltage and efficiency potential of emerging and established photovoltaic materials.

**Joeson Wong** orcid.org/0000-0002-6304-7602
**Stefan T. Omelchenko** orcid.org/0000-0003-1104-9291
**Harry A. Atwater** orcid.org/0000-0001-9435-0201

## ■ ASSOCIATED CONTENT

### Supporting Information

The Supporting Information is available free of charge at https://pubs.acs.org/doi/10.1021/acsenergylett.0c02362.


https://dx.doi.org/10.1021/acsenergylett.0c02362
ACS Energy Lett. 2021, 6, 52−57

Reciprocity relations background; calculation details; discussion of band-filling contribution and modified $J-V$ characteristics; discussion of two-bandgap model; derivation of generalized voltage loss mechanism and different band edge parametrizations; effects of different bandgaps, Urbach parameters, and thickness on photovoltaic figures of merit; effects of subunity radiative and quantum efficiencies; analysis of Gaussian tail distributions (PDF)

## AUTHOR INFORMATION

Complete contact information is available at:
https://pubs.acs.org/10.1021/acsenergylett.0c02362

### Author Contributions

J.W. and S.T.O. contributed equally. J.W. and S.T.O. developed the ideas and formulism and performed the calculations for all the results shown in this work. H.A.A supervised all the calculations and analysis. J.W. wrote the manuscript, with input from S.T.O and H.A.A. All authors contributed to the discussion and interpretation of results, as well as the presentation and preparation of the manuscript.

### Notes

Views expressed in this Viewpoint are those of the authors and not necessarily the views of the ACS.
The authors declare no competing financial interest.

## ACKNOWLEDGMENTS

This work is part of the "Photonics at Thermodynamic Limits" Energy Frontier Research Center funded by the U.S. Department of Energy, Office of Science, Office of Basic Energy Sciences under Award Number DE-SC0019140. J.W. acknowledges additional support from the National Science Foundation Graduate Research Fellowship under Grant No. 1144469.

## REFERENCES

(1) Shockley, W.; Queisser, H. J. Detailed Balance Limit of Efficiency of pn Junction Solar Cells. *J. Appl. Phys.* **1961**, *32* (3), 510−519.
(2) Blank, B.; Kirchartz, T.; Lany, S.; Rau, U. Selection Metric for Photovoltaic Materials Screening Based on Detailed-Balance Analysis. *Phys. Rev. Appl.* **2017**, *8* (2), 024032.
(3) Rau, U.; Blank, B.; Müller, T. C. M.; Kirchartz, T. Efficiency Potential of Photovoltaic Materials and Devices Unveiled by Detailed-Balance Analysis. *Phys. Rev. Appl.* **2017**, *7* (4), 1−9.
(4) Araújo, G. L.; Martí, A. Absolute Limiting Efficiencies for Photovoltaic Energy Conversion. *Sol. Energy Mater. Sol. Cells* **1994**, *33* (2), 213−240.
(5) Martí, A.; Araújo, G. L. Limiting Efficiencies for Photovoltaic Energy Conversion in Multigap Systems. *Sol. Energy Mater. Sol. Cells* **1996**, *43* (2), 203−222.
(6) Ross, R. T.; Nozik, A. J. Efficiency of Hot-Carrier Solar Energy Converters. *J. Appl. Phys.* **1982**, *53* (5), 3813−3818.
(7) Würfel, P. Solar Energy Conversion with Hot Electrons from Impact Ionisation. *Sol. Energy Mater. Sol. Cells* **1997**, *46* (1), 43−52.
(8) Xu, Y.; Gong, T.; Munday, J. N. The Generalized Shockley-Queisser Limit for Nanostructured Solar Cells. *Sci. Rep.* **2015**, *5*, 13536.
(9) Anttu, N. Shockley-Queisser Detailed Balance Efficiency Limit for Nanowire Solar Cells. *ACS Photonics* **2015**, *2* (3), 446−453.
(10) Klimov, V. I. Detailed-Balance Power Conversion Limits of Nanocrystal-Quantum-Dot Solar Cells in the Presence of Carrier Multiplication. *Appl. Phys. Lett.* **2006**, *89* (12), 123118.
(11) Hanna, M. C.; Nozik, A. J. Solar Conversion Efficiency of Photovoltaic and Photoelectrolysis Cells with Carrier Multiplication Absorbers. *J. Appl. Phys.* **2006**, *100* (7), 074510.
(12) Miller, O. D.; Yablonovitch, E.; Kurtz, S. R. Strong Internal and External Luminescence as Solar Cells Approach the Shockley-Queisser Limit. *Photovoltaics, IEEE J.* **2012**, *2* (3), 303−311.
(13) Urbach, F. The Long-Wavelength Edge of Photographic Sensitivity and of the Electronic Absorption of Solids. *Phys. Rev.* **1953**, *92* (5), 1324−1324.
(14) De Wolf, S.; Holovsky, J.; Moon, S.-J.; Loper, P.; Niesen, B.; Ledinsky, M.; Haug, F.-J.; Yum, J.-H.; Ballif, C. Organometallic Halide Perovskites: Sharp Optical Absorption Edge and Its Relation to Photovoltaic Performance. *J. Phys. Chem. Lett.* **2014**, *5*, 1035−1039.
(15) Kurik, M. V. Urbach Rule. *Phys. Status Solidi Appl. Mater. Sci.* **1971**, *8* (1), 9.
(16) John, S.; Soukoulis, C.; Cohen, M. H.; Economou, E. N. Theory of Electron Band Tails and the Urbach Optical-Absorption Edge. *Phys. Rev. Lett.* **1986**, *57* (14), 1777−1780.
(17) Sritrakool, W.; Sa-yakanit, V.; Glyde, H. R. Band Tails in Disordered Systems. *Phys. Rev. B: Condens. Matter Mater. Phys.* **1986**, *33* (2), 1199−1202.
(18) Cody, G. D.; Tiedje, T.; Abeles, B.; Brooks, B.; Goldstein, Y. Disorder and the Optical-Absorption Edge of Hydrogenated Amorphous Silicon. *Phys. Rev. Lett.* **1981**, *47* (20), 1480−1483.
(19) Johnson, S. R.; Tiedje, T. Temperature Dependence of the Urbach Edge in GaAs. *J. Appl. Phys.* **1995**, *78* (9), 5609−5613.
(20) Nayak, P. K.; Mahesh, S.; Snaith, H. J.; Cahen, D. Photovoltaic Solar Cell Technologies: Analysing the State of the Art. *Nat. Rev. Mater.* **2019**, *4* (4), 269−285.
(21) Katahara, J. K.; Hillhouse, H. W. Quasi-Fermi Level Splitting and Sub-Bandgap Absorptivity from Semiconductor Photoluminescence. *J. Appl. Phys.* **2014**, *116* (17), 173504.
(22) Jean, J.; Mahony, T. S.; Bozyigit, D.; Sponseller, M.; Holovský, J.; Bawendi, M. G.; Bulović, V. Radiative Efficiency Limit with Band Tailing Exceeds 30% for Quantum Dot Solar Cells. *ACS Energy Lett.* **2017**, *2* (11), 2616−2624.
(23) Rau, U.; Werner, J. H. Radiative Efficiency Limits of Solar Cells with Lateral Band-Gap Fluctuations. *Appl. Phys. Lett.* **2004**, *84* (19), 3735−3737.
(24) Chuang, C. H. M.; Maurano, A.; Brandt, R. E.; Hwang, G. W.; Jean, J.; Buonassisi, T.; Bulović, V.; Bawendi, M. G. Open-Circuit Voltage Deficit, Radiative Sub-Bandgap States, and Prospects in Quantum Dot Solar Cells. *Nano Lett.* **2015**, *15* (5), 3286−3294.
(25) Gokmen, T.; Gunawan, O.; Todorov, T. K.; Mitzi, D. B. Band Tailing and Efficiency Limitation in Kesterite Solar Cells. *Appl. Phys. Lett.* **2013**, *103* (10), 103506.
(26) Parrott, J. E. Self-Consistent Detailed Balance Treatment of the Solar Cell. *IEE Proc.-J: Optoelectron.* **1986**, *133* (5), 314−318.
(27) Wurfel, P. The Chemical Potential of Radiation. *J. Phys. C: Solid State Phys.* **1982**, *15* (18), 3967−3985.
(28) Bhattacharya, R.; Pal, B.; Bansal, B. On Conversion of Luminescence into Absorption and the van Roosbroeck-Shockley Relation. *Appl. Phys. Lett.* **2012**, *100* (22), 222103.
(29) Nguyen, D. T.; Lombez, L.; Gibelli, F.; Boyer-Richard, S.; Le Corre, A.; Durand, O.; Guillemoles, J. F. Quantitative Experimental Assessment of Hot Carrier-Enhanced Solar Cells at Room Temperature. *Nat. Energy* **2018**, *3* (3), 236−242.
(30) Gibelli, F.; Lombez, L.; Guillemoles, J. F. Accurate Radiation Temperature and Chemical Potential from Quantitative Photoluminescence Analysis of Hot Carrier Populations. *J. Phys.: Condens. Matter* **2017**, *29* (6), 06LT02.
(31) Rau, U. Reciprocity Relation between Photovoltaic Quantum Efficiency and Electroluminescent Emission of Solar Cells. *Phys. Rev. B: Condens. Matter Mater. Phys.* **2007**, *76* (8), 1−8.
(32) Liu, S.; Yuan, J.; Deng, W.; Luo, M.; Xie, Y.; Liang, Q.; Zou, Y.; He, Z.; Wu, H.; Cao, Y. High-Efficiency Organic Solar Cells with Low Non-Radiative Recombination Loss and Low Energetic Disorder. *Nat. Photonics* **2020**, *14* (May), 300.

(33) Baran, D.; Kirchartz, T.; Wheeler, S.; Dimitrov, S.; Abdelsamie, M.; Gorman, J.; Ashraf, R. S.; Holliday, S.; Wadsworth, A.; Gasparini, N.; Kaienburg, P.; Yan, H.; Amassian, A.; Brabec, C. J.; Durrant, J. R.; McCulloch, I. Reduced Voltage Losses Yield 10% Efficient Fullerene Free Organic Solar Cells with > 1 V Open Circuit Voltages. *Energy Environ. Sci.* **2016**, *9* (12), 3783−3793.
(34) Qian, D.; Zheng, Z.; Yao, H.; Tress, W.; Hopper, T. R.; Chen, S.; Li, S.; Liu, J.; Chen, S.; Zhang, J.; Liu, X. K.; Gao, B.; Ouyang, L.; Jin, Y.; Pozina, G.; Buyanova, I. A.; Chen, W. M.; Inganäs, O.; Coropceanu, V.; Bredas, J. L.; Yan, H.; Hou, J.; Zhang, F.; Bakulin, A. A.; Gao, F. Design Rules for Minimizing Voltage Losses in High-Efficiency Organic Solar Cells. *Nat. Mater.* **2018**, *17* (8), 703−709.
(35) Ran, N. A.; Love, J. A.; Takacs, C. J.; Sadhanala, A.; Beavers, J. K.; Collins, S. D.; Huang, Y.; Wang, M.; Friend, R. H.; Bazan, G. C.; Nguyen, T. Q. Harvesting the Full Potential of Photons with Organic Solar Cells. *Adv. Mater.* **2016**, *28* (7), 1482−1488.


https://dx.doi.org/10.1021/acsenergylett.0c02362
*ACS Energy Lett.* 2021, 6, 52−57